DOI: 10.1002/ejic.200700356

Synthesis and Characterisation of Semi-Bridging Molybdenum Borylene Complexes

Holger Braunschweig,*[a] Krzysztof Radacki,[a] and Katharina Uttinger[a]

Keywords: Boron / Borylene complexes / Molybdenum / Palladium / DFT calculations

Investigation of the reactivity of the molybdenum borylene complex $[(OC)_5Mo{=}B{=}N(SiMe_3)_2]$ towards the late transition metal complexes $[M(PCy_3)_2]$ (M = Pd, Pt) indicated the formation of $[(OC)_4Mo(\mu\text{-}CO)\{\mu\text{-}BN(SiMe_3)_2\}Pd(PCy_3)]$ and $[(Cy_3P)(OC)_3Mo(\mu\text{-}CO)\{\mu\text{-}BN(SiMe_3)_2\}Pt(PCy_3)]$, respectively, as the first Mo-based semi-bridging borylene complexes. The new complexes were fully characterised spectroscopically and analysed by X-ray diffraction. The conclusions drawn from the experimental data for the ligand-metal interactions for this particular coordination mode of a borylene group were supported by DFT computations.

Transition metal boryl complexes have attracted significant interest due to their role as key intermediates in catalysed hydro-[1] and diboration reactions[2] as well as in C–H bond activation of organic compounds.[3] Borylene complexes as another type of metal-boron compound are also in the focus of research[4] because of their close relationship to carbonyl complexes and due to their propensity to effectively stabilise[4g,5] elusive borylenes[6] in the coordination sphere of a metal. In particular, group 6 transition metal carbonyl fragments have been shown to possess good stabilising properties resulting in the formation, by means of a salt elimination reaction, of $[(OC)_5M{=}B{=}N(SiMe_3)_2]$ (M = Cr, **1**; W, **2**) which are the first two-coordinate borylene complexes.[7] Unfortunately, this method of preparation is limited in scope and, hence, the borylene transfer under thermal[8] or photochemical conditions[9] has become established as a highly useful alternative for the synthesis of borylene complexes and borylene functionalised main group element substrates.[10]

Very recently, it was demonstrated that borylene ligands (Figure 1) can adopt rather unusual coordination modes beyond the common scope of mononuclear neutral (e.g. **1**, **2** and **3**)[7,9,11] and cationic (e.g. **4**)[12] or symmetrically bridged homodinuclear species (e.g. **5** and **6**).[9a,13] Important examples include heterodinuclear borylene complexes (e.g. **7**),[14] metalloborylenes (e.g. **8**)[8d,15] (Figure 1) and dinuclear compounds with semi-bridging borylene ligands.[8a,8b]

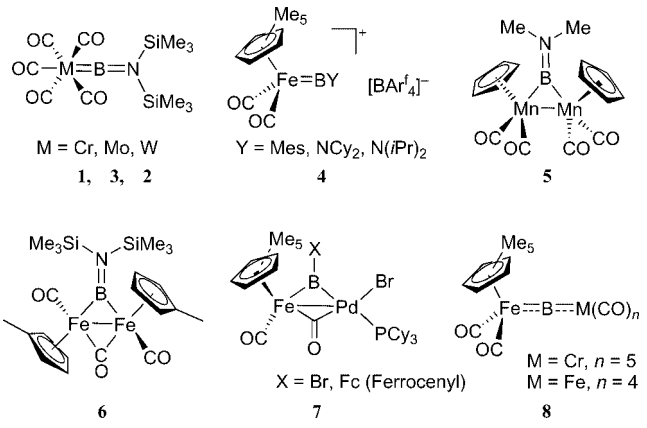

Figure 1. Different coordination modes for borylene ligands: terminal **1**,[7,9a] **2**[7] and **3**,[11b] cationic **4**,[12a,12b,12c] symmetrically bridging homodinuclear **5**[13a] and **6**,[13b] symmetrically bridging heterdionuclear **7**[14] and metalloborylene **8**.[15]

In the case of the group 6 transition metals, several boryl and borylene complexes of tungsten are known for example $[L(OC)_4W{=}B{=}N(SiMe_3)_2]$ (L = CO, **2**; PCy_3)[7,11b] and $[(\eta^5\text{-}C_5H_5)_2WXBR_2]$ (X = H, R_2 = Ph_2, 1,2-O_2-C_6H_4; X = Cl, R_2 = 1,2-O_2-C_6H_4),[16] $[(\eta^5\text{-}C_5H_5)_2W(BR_2)_2]$ [R_2 = (1,2-O_2-4-*t*BuC_6H_3), (1,2-O_2-3,5-*t*$Bu_2C_6H_2$)][16b,17] or $[(\eta^5\text{-}C_5H_5)\text{-}W(CO)_3\{B(NMe_2)B(NMe_2)X\}]$ (X = Cl, Br, I),[18] most of them being fully characterised including crystallographic data. Likewise, a variety of chromium borylene complexes were reported, e.g. $[L(OC)_4Cr{=}B{=}N(SiMe_3)_2]$ (L = CO, **1**; PCy_3, **10**),[7,8a,9a,11b] $[(OC)_5Cr{=}B{-}Si(SiMe_3)_3]$[11a] and $[(OC)_5\text{-}Cr{=}B{-}Fe(\eta^5\text{-}C_5H_5)(CO)_2]$ (**8**)[15] and in addition, one boryl complex $[Cr(\eta^6\text{-}C_6H_6)(CO)_2(\eta^2\text{-}tmp'BCR_2)]$ [$tmp'BCR_2$ = (η^2-9-fluorenylidene)(2,2,6,6-tertramethylpiperidino)-borane].[19] In the case of molybdenum, however, only few boryl complexes of molybdenum are known, e.g.

[a] Institut für Anorganische Chemie, Julius-Maximilians-Universität Würzburg,
Am Hubland, 97074 Würzburg, Germany
Fax: +49-931-888-4623
E-mail: h.braunschweig@mail.uni-wuerzburg.de

Supporting information for this article is available on the WWW under http://www.eurjic.org or from the author.

[Mo(tpb′)(CO)$_2${B(Et)CH$_2$-*p*-tolyl}] [tpb′ = tris(3,5-dimethylpyrazol-1-yl)hydroborate][20] or the diborane(4)yl complex [(η^5-C$_5$H$_5$)Mo(CO)$_3${B(NMe$_2$)B(NMe$_2$)X}] (X = Br, I)[18b,18c,18d] and only very recently we contributed the first Mo borylene complex [(OC)$_5$Mo=B=N(SiMe$_3$)$_2$] (**3**) and reported its conversion to *trans*-[(Cy$_3$P)(OC)$_4$-Mo=B=N(SiMe$_3$)$_2$] (**11**).[11b] Presumably, the relative scarcity of Mo–boron complexes can be attributed to the enhanced lability of 4d transition metal complexes with respect to their corresponding 3d and 5d analogues.[21]

Recent studies have shown that metal coordinated borylene and, albeit to a lesser extent, boryl ligands[22] are highly susceptible to the addition of transition metal bases, leading in the case of the former to novel heterodi- and trinuclear borylene species.[8c,8d]

In this paper we report on the reactivity of [(OC)$_5$-Mo=B=N(SiMe$_3$)$_2$] (**3**)[11b] towards the late transition metal complexes [M(PCy$_3$)$_2$] (M = Pd, **12**; Pt, **13**)[23] which leads to the first Mo-species comprised of a semi-bridging borylene ligand. In addition, we provide detailed results of DFT studies which have elucidated the electronic structures of the title compounds.

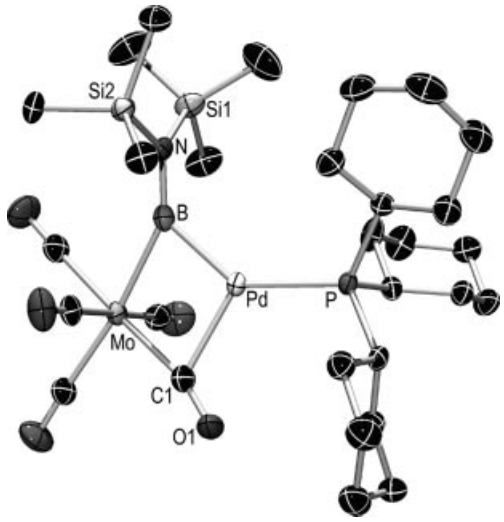

Figure 2. Molecular structure of [(OC)$_4$Mo(μ-CO){μ-BN(SiMe$_3$)$_2$}Pd(PCy$_3$)] (**16**). Thermal ellipsoids are set at the 50% probability level. Selected bond lengths [Å] and angles [°]: Mo–B 2.235(4), Pd–B 2.065(4), B–N 1.376(5), Pd–P 2.3764(9), Pd–Mo–C1 51.74(10), Mo–C1–O1 164.3(3), Pd–Mo–B 47.59(10), Mo–B–N 150.7(3), Si1–N–B–Pd 86.1(3).

Results and Discussion

Equimolar amounts of [(OC)$_5$Mo=B=N(SiMe$_3$)$_2$] (**3**) and [Pd(PCy$_3$)$_2$] (**12**) were mixed in C$_6$D$_6$ at room temperature. The progress of the reaction was monitored by multinuclear NMR spectroscopy and, after 30 min, complete conversion of the starting materials, formation of a new compound and liberation of PCy$_3$ [δ (^{31}P) = 10.0 ppm] was observed. The product was isolated as orange crystals in 53% yield by layering a toluene solution with hexane and storing at –35 °C overnight. The ^{11}B{^{1}H} NMR spectrum shows a broad signal at δ = 99 ppm which is downfield shifted with respect to that in the precursor **3** (δ = 89.7 ppm).[11b] A sharp resonance at δ = 35.1 ppm in the ^{31}P{^{1}H} NMR spectrum can be observed for the metal coordinated phosphane ligand indicating the presence of only one tricyclohexylphosphane unit in the molecule. The ^{1}H NMR spectrum features one singlet for both trimethylsilyl groups at δ = 0.41 ppm which is deshielded with respect to that of the borylene precursor **3** (δ = 0.15 ppm)[11b] but comparable to those of the Cr and W analogues ([(OC)$_4$-M(μ-CO){μ-BN(SiMe$_3$)$_2$}Pd(PCy$_3$)], M = Cr, **14**; M = W, **15**; δ = 0.42 ppm).[10a]

The result of a single-crystal X-ray diffraction study of [(OC)$_4$Mo(μ-CO){μ-BN(SiMe$_3$)$_2$}Pd(PCy$_3$)] (**16**) is shown in Figure 2.

Compound **16** crystallises in the orthorhombic space group *Pna*2$_1$ with the two metal fragments [Mo(CO)$_4$] and [Pd(PCy$_3$)] linked by a bridging CO and a –BN(SiMe$_3$)$_2$ group. The latter is oriented almost perpendicular with respect to the plane containing Mo, B and Pd as indicated by the dihedral angle Si1–N–B–Pd of 86.1(3)°. The Mo–B bond [2.235(4) Å] is elongated by 8 pm when compared with the terminal Mo-borylene complex **3** [2.1519(15) Å][11b] and this is due to the increased coordination number of the boron centre in the former. However, it is still shorter (10 pm) than the distance in the only structurally characterised complex with a Mo–B–bond [(η^5-C$_5$H$_5$)Mo(CO)$_2$-COB(NMe$_2$)B(NMe$_2$)Mo(CO)$_3$] [Mo–B 2.348(4) Å].[18b,18c] Likewise, the Pd–B bond length [2.065(4) Å] lies within the expected range for three-coordinate boron linked to a palladium centre [2.006(9)–2.077(6) Å].[24] The relatively short B–N distance of 1.376(5) Å, which is only marginally longer than in the corresponding borylene complex **3** [1.3549(18) Å], indicates significant double bond character in the B–N linkage.[11b] In contrast, the homodinuclear bridged aminoborylene species [{(η^5-C$_5$H$_5$)Mn(CO)$_2$}$_2${μ-BNMe$_2$}] (**5**)[13a] and [{(η^5-C$_5$H$_4$Me)Fe(CO)}$_2$(μ-CO){μ-BN(SiMe$_3$)$_2$}] (**6**),[13b] in which the boron centres possess formal sp^2 hybridisation, display a different arrangement. In **5** the B–N distance of 1.39(1) Å is also in agreement with the formulation of a B=N double bond, the plane of the BNMe$_2$ substituent, however, is arranged almost coplanar [8(3)°] with respect to the Mn$_2$B plane[13a] whereas in **6** the BN(SiMe$_3$)$_2$ plane is twisted by 53(1)° with respect to the Fe$_2$B plane resulting in less effective N–B π bonding and, hence, an elongation of the B–N bond [1.412(4) Å].[13b] The perpendicular disposition of the two respective planes in **16** in combination with a typical B–N double bond length disagrees with the description of a formally sp^2 hybridised boron centre. More appropriate is the description of the overall bonding situation in terms of a terminal borylene centre being stabilised by a metal base. The Lewis-basic [(Cy$_3$P)Pd] fragment releases electron density into the empty orbitals of CO and the borylene moiety (vide infra). Thus, the π acceptor fragments CO and BN(SiMe$_3$)$_2$ form a pair of two noncompensating, semi-bridging ligands. The classification scheme for semi-bridging carbonyl ligands de-

veloped by Crabtree[25] is applicable to the relevant bond angles [Pd–Mo–C1 51.74(10)°; Mo–C1–O1 164.3(3)°]. The corresponding angles for the semi-bridging B–R moiety [Pd–Mo–B 47.59(10)°; Mo–B–N 150.7(3)°] lie clearly between those typically found for terminal and symmetrically bridging ligands and are similar to their semi-bridging Cr and W analogues **14** and **15**.[10a]

For the synthesis of **16**, it is important to restrict the reaction time to a minimum since liberated phosphane tends to substitute a carbonyl group at Mo which subsequently leads to formation of a variety of degradation products as indicated by $^{31}P\{^1H\}$ NMR spectroscopic data: $[(Cy_3P)(OC)_3Mo(\mu\text{-}CO)\{\mu\text{-}BN(SiMe_3)_2\}Pd(PCy_3)]$ (**17**) [δ (^{31}P) = 50.7 ppm (d, $^4J_{P,P}$ = 12 Hz, P_{Mo}), 33.9 ppm (d, $^4J_{P,P}$ = 12 Hz, P_{Pd}); δ (^1H) = 0.63 ppm (s, $SiMe_3$)], *trans*-$[(Cy_3P)(OC)_4Mo{=}BN(SiMe_3)_2]$ (**11**) [δ (^{31}P) = 51.2 ppm (s); δ (^1H) = 0.37 ppm (s, $SiMe_3$)],[11b] and $[(OC)_5Mo(PCy_3)]$ (**18**) [δ (^{31}P) = 47.8 ppm(s)]. In a typical experiment, a ratio of 9:1 for $[(OC)_4Mo(\mu\text{-}CO)\{\mu\text{-}BN(SiMe_3)_2\}Pd(PCy_3)]$ (**16**) to $[(Cy_3P)(OC)_3Mo(\mu\text{-}CO)\{\mu\text{-}BN(SiMe_3)_2\}Pd(PCy_3)]$ (**17**) was observed after 30 min which decreased after 1 d to 3:1 and, in addition, *trans*-$[(Cy_3P)(OC)_4Mo{=}BN(SiMe_3)_2]$ (**11**) started to be formed. Finally, after 4 d the ratio was approximately 4:3:3 according to the ^1H NMR spectra.

In order to study whether *trans*-$[(Cy_3P)(OC)_4Mo{=}BN(SiMe_3)_2]$ (**11**) is available in an analogous manner to the Cr complex **10** by irradiation of the heterodinuclear complex **14**,[10a] $[(OC)_4Mo(\mu\text{-}CO)\{\mu\text{-}BN(SiMe_3)_2\}Pd(PCy_3)]$ (**16**) was photolysed. According to the $^{31}P\{^1H\}$ NMR spectra, however, the aforementioned product mixture of **16**, **17**, **11** and **18** was already obtained after 30 min but now with a ratio of 5:4:6:14.

In order to complete the series of semi-bridging group 6 borylene complexes with Pd- and Pt-base stabilisation, $[(OC)_5Mo = BN(SiMe_3)_2]$ (**3**) was treated with $[Pt(PCy_3)_2]$ (**13**) in C_6D_6 under identical conditions. The reaction mixture showed several compounds, from which $[(Cy_3P)(OC)_3Mo(\mu\text{-}CO)\{\mu\text{-}BN(SiMe_3)_2\}Pt(PCy_3)]$ (**19**), *trans*-$[(Cy_3P)(OC)_4Mo{=}BN(SiMe_3)_2$ (**11**), $[(OC)_5Mo(PCy_3)]$ (**18**) and PCy_3 could be identified by $^{31}P\{^1H\}$ NMR spectroscopy. The dinuclear complex **19** was isolated by layering a toluene solution with hexane and slow evaporation of the solvent.

The $^{31}P\{^1H\}$ NMR spectrum of the isolated compound **19** showed two doublets [δ = 70 ppm (d, $^4J_{P,P}$ = 11 Hz, $^1J_{P,Pt}$ = 5002 Hz, P_{Pt}), 49.9 (d, $^4J_{P,P}$ = 11 Hz, $^3J_{P,Pt}$ = 73 Hz, P_{Mo})], indicating the presence of two nonequivalent phosphane ligands. A singlet for the $-SiMe_3$ groups (δ = 0.63 ppm) in the ^1H NMR spectrum as well as a broad resonance in the $^{11}B\{^1H\}$ NMR spectrum (δ = 100 ppm) were observed downfield shifted with respect to the signals of the starting material **3**.[11b] The reaction with $[Pt(PCy_3)_2]$ (**13**) proceeds even faster than that with $[Pd(PCy_3)_2]$ (**12**), or the one of **13** with the W-borylene **2**.[10b] Therefore, very fast work-up is required, since the NMR spectroscopic data recorded 1 h after mixing the reactants already indicated a 2:2:1 mixture of the subsequently isolated product $[(Cy_3P)(OC)_3Mo(\mu\text{-}CO)\{\mu\text{-}BN(SiMe_3)_2\}Pt(PCy_3)]$ (**19**), the borylene complex *trans*-$[(Cy_3P)(OC)_4Mo{=}BN(SiMe_3)_2]$ (**11**)[11b] and $[(Cy_3P)Mo(CO)_5]$ (**18**) (Scheme 1). After one week, the ratio has changed to 1:2:2, thus explaining the low yield of 12%.

The molecular constitution of **19** was determined by a single-crystal X-ray diffraction study (see Figure 3). The complex crystallises in the triclinic space group $P\bar{1}$ and

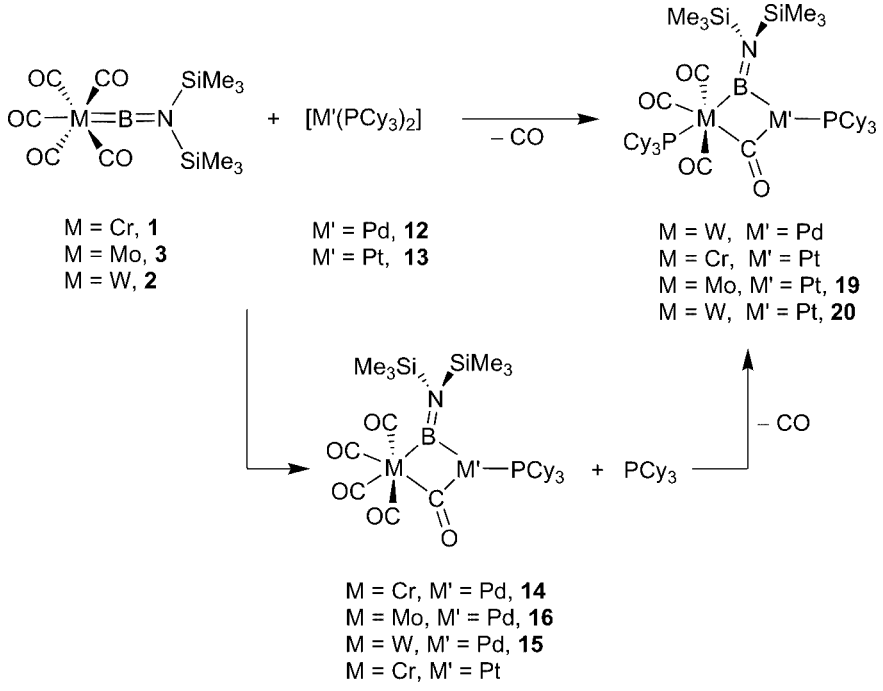

Scheme 1. Survey for the reaction mechanism of the formation of different semi-bridging borylene complexes.

shows similar structural features to the W analogue **20**[10b] or the Mo–Pd compound **16** particularly with respect to the geometries of the CO [Pt–Mo–C1 51.38(14)°; Mo–C1–O1 165.7(4)°] and borylene ligands [Pt–Mo–B 49.34(15)°; Mo–B–N 153.2(4)°]. These data together with the short B=N double bond [1.408(7) Å] and the orthogonal orientation of the aminoborylene group with respect to the M–B–Pt plane [Si2–N–B–Mo 91.2(9)°] demonstrate the presence of semi-bridging borylene and CO ligands, respectively. Comparison of the Mo–B bond lengths in the mono- and diphosphane complexes **16** and **19**, however, reveals distinct differences. In the case of **19**, the Mo–B separation of 2.138(6) Å is significantly smaller than that in **16** [2.235(4) Å] but falls barely below the Mo–B distance in **3** [2.1519(15) Å][11b] despite the higher coordination number of the boron atom in the diphosphane complex **19**. The same effect has already been observed in the corresponding complexes of W (**15** and **20** in comparison with **2**).[10b] Clearly, the presence of the PCy_3 group in a *trans* position to the borylene leads to a decreased M–B separation due to the reduced π acceptor abilities of the phosphane when compared with CO, thus inducing a stronger M–B d_π–p_π back donation. A similar observation was made in the case of terminal borylene complexes **1**–**3**, substituted with a phosphane ligand in *trans* position to the boron atom [*trans*-[$(Cy_3P)(OC)_4$M=BN$(SiMe_3)_2$] (M = Cr, **9**; Mo, **11**; W, **10**)].[10b,11b]

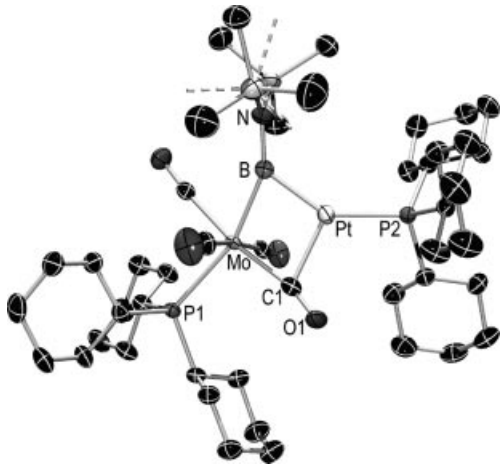

Figure 3. Molecular structure of [$(Cy_3P)(OC)_3$Mo(μ-CO){μ-BN$(SiMe_3)_2$}Pt(PCy_3)] (**19**). Thermal ellipsoids are set at the 50% probability level Selected bond lengths [Å] and angles [°]: B–N 1.408(7), Mo–B 2.138(6), Pt–P2 2.2912(13), Mo–P1 2.5587(12), Pt–Mo–C1 51.38(14), Mo–C1–O1 165.7(4), Pt–Mo–B 49.34(15), Mo–B–N 153.2(4), Si2–N–B–Mo 91.2(9).

Calculations

To gain some deeper insight into the electronic structures of semi-bridging borylene complexes, we performed DFT computations on model systems of the complexes **16**, **17** and **19**.[26] Since no significant difference was observed between the Pd and Pt analogues, only the results for the Pd complexes are presented. To reduce computation time PMe_3 was used instead of PCy_3 and $N(SiMe_3)_2$ was replaced by $N(SiH_3)_2$.

To our surprise, the optimised geometry of the model compound [$(OC)_4$Mo(μ-CO){μ-BN$(SiH_3)_2$}Pd(PMe_3)] (**16a**) displays a Si–N–B–Mo torsion angle of ca. 41°. Reoptimisation with the smaller NH_2 group (**16b**$_{Min}$) led to the coplanar system $C_\mu M_2B{=}NH_2$, thus allowing π interaction between the electron lone pair on the nitrogen and the empty p orbital of the boron atom to extend to both metal atoms, thus providing evidence that the mutual orthogonal orientation of the amino-group and the four-membered ring $C_\mu M_2B$ is caused by steric effects. The molecule with an orthogonal disposition of the two respective planes was found to be a transition state (**16b**$_{TS}$) on the PES which is 34.4 kJ mol^{-1} higher in energy than the coplanar minimum structure **16b**$_{Min}$.

As mentioned before, the B–N bond in **16** is only negligibly longer than that in the terminal borylene **3** (137.6 vs. 135.5 pm). The DFT computations for **16b**$_{Min}$ and **16b**$_{TS}$ result in very similar B–N distances (138.5 and 139.9 pm respectively) thus mirroring the short experimental B–N bond despite the orthogonal orientation of the amino-group to the BM_2 plane. The arguments against sp^2 hybridisation of boron were already raised in the crystal structure discussion and are supported by theory. Even for **16b**$_{TS}$ with its orthogonally orientated amino-group, one can identify an orbital clearly describing the B=N π interaction (HOMO–8), thus backing up the relative high s character of the hybrid orbital at the boron atom (see Figure 4).

We analysed the canonical orbitals of the parent compound **16b**$_{TS}$ with regards to interaction between the Mo borylene moiety [$(OC)_5MoBNH_2$] and the metal base [$Pd(PH_3)$]. For this analysis the transition state geometry **16b**$_{TS}$ rather than the minimum **16b**$_{Min}$ was employed since it displays the same orientation for the amino group as that found experimentally for **16**. Selected orbitals for **16b**$_{TS}$ are depicted in Figure 4.

The HOMO-9 and HOMO-10 are characterised mainly by σ interaction between the lone pair of the formal borylene BNH_2 and d orbitals of palladium. The HOMO-7 is primarily composed of a palladium d_{xz} + d_{yz} hybrid (ca. 2:1) orbital with some admixture of the boron p_z orbital and thus describes the Pd→B π backbonding interaction. Inspection of the orbitals revealed, that in spite of similarities between borylenes and carbonyls, there is a difference in their interaction with metal bases. Marder et al. employed the Fragment Orbital Analysis for [(η^5-C_5H_5)(OC)Rh(μ-CO)$_2$Cr(CO)(C_6H_6)] and found that the dominant interaction between the metal-base [(η^5-C_5H_5)(OC)Rh] and the metal-carbonyl fragment [$(OC)_3$Cr(η^6-C_6H_6)] is that of occupied d orbitals of rhodium with unoccupied π* orbitals on the carbonyl groups. In the case of the borylene, however, the HOMO-3 shows no bonding character between the boron and metal centre because the hybrid orbital on boron is a mixture of p_y and p_x with s orbitals. Mixing of both p functions adjusts the direction of the hybrid towards molybdenum and subtraction of the s function removes a lobe pointing toward palladium and leads to further polari-

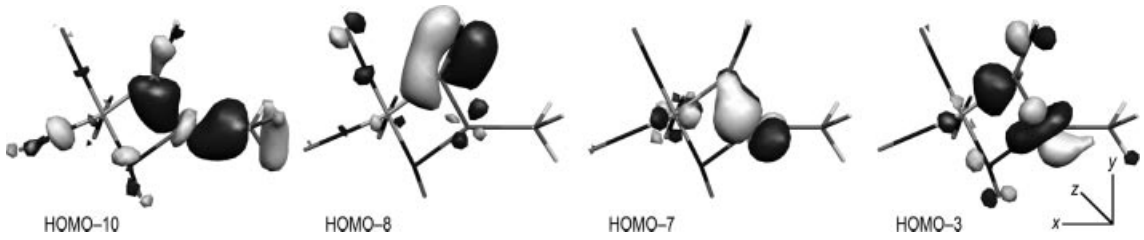

Figure 4. Kohn–Sham orbitals of $[(OC)_4Mo(\mu\text{-}CO)(\mu\text{-}BNH_2)Pd(PH_3)]$ **16b**$_{TS}$.

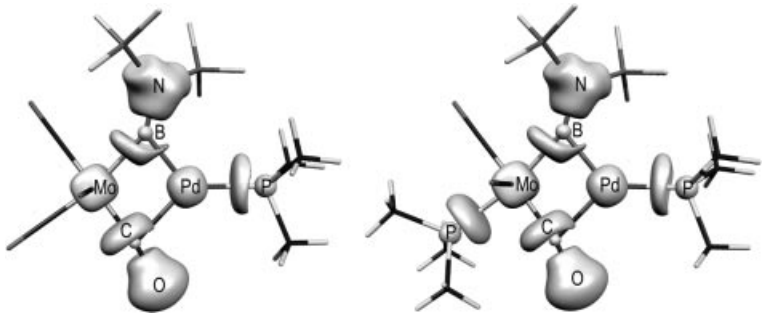

Figure 5. Plot of the ELF (isosurface: 0.70) of $[(OC)_4Mo(\mu\text{-}CO)\{\mu\text{-}BN(SiH_3)_2\}Pd(PMe_3)]$ **16a** and $[(Me_3P)(OC)_3Mo(\mu\text{-}CO)\{\mu\text{-}BN(SiH_3)_2\}Pd(PMe_3)]$ **17a**. The ELF surface around the ligands has been omitted for clarity.

sation towards Mo. The interaction of the Pd-fragment with the unoccupied orbital of the carbonyl group plays only a minor role as also indicated by the experimental data, i.e. the Pd–C_μ distance is significantly greater than the Pd–B separation.

Analysis of the Electron Localisation Function (ELF) can provide insight into the topology of valence electron pairs. Similar to $[(\mu_3\text{-}BMe)\{[(\eta^5\text{-}C_5H_5)Mn(CO)_2][Pd(PMe_3)]_2\}]$,[8c–8d] ELF computations located, in all computed molecules, three-synaptic basins representing (3c,2e)–Mo–B–Pd bonds, with their attractors localised on the boron-metal side. The situation of the bridging carbonyls resembles that of the borylenes. The ELF attractors of the Mo–C–Pd basins are also placed between Mo and the bridging atom (see Figure 5). In all cases the highest atomic contribution to the three-synaptic basins is provided by the central atom (ca. 50%).

The shape of the ELF basins of **16a** is very similar to that of $[(Me_3P)(OC)_3Mo(\mu\text{-}CO)\{\mu\text{-}BN(SiH_3)_2\}Pd(PMe_3)]$ (**17a**). There is, however, a distinct discrepancy in the population of the B–N disynaptic basins which illustrates the difference in the *trans* effect of carbonyl vs. the phosphane groups. Formal exchange of CO in **17a** by a phosphane leads to a stronger Mo–B interaction, thus resulting in weaker B=N and B–Pd bonds. This phenomenon is reflected in the values of the Wiberg Bond Index (WBI). The WBI of the B–Mo bonds increases from 0.59 to 0.76 while at the same time it decreases for the B–Pd bonds from 0.61 to 0.53 when compared **16a** with **17a**. It should be mentioned, that despite short interatomic distances, neither ELF attractors nor the WBI indicates a distinct Mo–Pd interaction (see Table 1).

Table 1. Analysis of bonding in $[(OC)_4Mo(\mu\text{-}CO)(\mu\text{-}BNH_2)Pd(PH_3)]$ (**16b**$_{Min}$ and **16b**$_{TS}$) $[(OC)_4Mo(\mu\text{-}CO)\{\mu\text{-}BN(SiH_3)_2\}Pd(PMe_3)]$ (**16a**), and $[(Me_3P)(OC)_3Mo(\mu\text{-}CO)\{\mu\text{-}BN(SiH_3)_2\}Pd(PMe_3)]$ (**17a**).

	16b$_{Min}$	**16b**$_{TS}$	**16a**	**17a**
Bond lengths [pm] and angles [°]				
$\angle(M_2BC)(R_2NB)$	0.0	90.0	41.0	39.2
B–Mo	224.5	224.2	226.4	217.4
B–Pd	204.3	203.8	204.8	210.0
C_μ–Mo	207.2	208.2	207.8	207.6
C_μ–Pd	236.4	236.0	233.4	227.5
B=N	138.5	139.9	139.9	140.9
N–B–Mo	146.3	150.2	149.2	153.1
Mo–B–Pd	82.2	82.1	81.5	81.8
Wiberg Bond Indices				
B–Mo	0.61	0.63	0.59	0.76
B–Pd	0.62	0.58	0.61	0.53
C_μ–Mo	0.76	0.74	0.74	0.75
C_μ–Pd	0.21	0.22	0.24	0.28
B=N	1.13	1.03	1.01	0.98
Mo–Pd	0.11	0.11	0.11	0.12
Natural charges				
B	0.54	0.62	0.61	0.64
Mo	–1.17	–1.20	–1.17	–1.20
Pd	0.06	0.02	0.01	0.01
C_μ	0.51	0.51	0.51	0.49
ELF basin population				
B=N	3.92	3.97	3.47	2.67
Mo–B–Pd	3.13	3.13	3.23	3.22
Mo–C–Pd	3.08	3.15	3.15	3.20

Conclusions

The first Mo-based semi-bridging borylene complexes $[(OC)_4Mo(\mu\text{-}CO)\{\mu\text{-}BN(SiMe_3)_2\}Pd(PCy_3)]$ (**16**) and $[(Cy_3P)(OC)_3Mo(\mu\text{-}CO)\{\mu\text{-}BN(SiMe_3)_2\}Pt(PCy_3)]$ (**19**) were ob-

tained from the reaction of $[(OC)_5Mo{=}B{=}N(SiMe_3)_2]$ (**3**) with the late transition metal complexes $[M(PCy_3)_2]$ (M = Pd, **12**; Pt, **13**) and fully characterised in solution and in the crystalline state. As indicated by multinuclear NMR spectroscopy, the formation of these heterodinuclear species is induced by cleavage of PCy_3 from the Pd and Pt precursors and subsequent addition of the Lewis-basic metal fragments $[M(PCy_3)]$ to the borylene moiety, thus representing a rare case of reactivity of terminal aminoborylene complexes under thermal (i.e. nonphotolytic) conditions. The generally increased lability of Mo organometallics with respect to their Cr and W counterparts is reflected by the rapid formation of the borylene species reported here and, in particular, by their enhanced reactivity, thus leading to the formation of a variety of side and degradation products. This, above all, is true for the instantaneous generation of the diphosphane complex **19** which is supposedly formed via a monophosphane intermediate $[(OC)_4M(\mu\text{-}CO)\{\mu\text{-}BN(SiMe_3)_2\}Pt(PCy_3)]$ analogous to **16** and which is known for M = Cr and W but could not be detected here in the case of M = Mo. Besides, this facile substitution of CO by PCy_3 provides further evidence of the strong *trans* influence of boron centred ligands.

The particular coordination mode of the aminoborylene ligand in the title compounds was elucidated for the first time by detailed DFT and ELF studies which demonstrated, in agreement with the structural data, that the $(Me_3Si)_2NB$ moiety adopts a semi-bridging position which is well known for related carbonyl complexes but has only very recently started to appear for borylenes. From the computational data it can be concluded that the $(Me_3Si)_2NB$ ligand is characterised by a pronounced B=N double bond and a predominantly sp hybridised boron atom and donates σ electron density from its formal lone pair to both metal centres and receives in return π back donation into a p_z orbital. In addition, structural and computational data indicate that a phosphane group *trans* to the semi-bridging borylene (e.g. **19**) increases the Mo–B bond strength with respect to a *trans* CO ligand, due to the higher π acceptor abilities of the latter.

Experimental Section

All manipulations were performed either under an atmosphere of dry argon or in vacuo using standard Schlenk line and glove-box techniques. Solvents were dried by standard methods and were distilled and stored over molecular sieves prior to use. Deuterated solvents (C_6D_6) were degassed by three freeze-pump-thaw cycles and stored over molecular sieves in the glove-box. The irradiation experiments were carried out using a Heraeus TQ 150 high-pressure Hg lamp. IR spectra were recorded as toluene solutions between NaCl plates on a Bruker Vector 22 FTIR spectrometer. NMR spectra were acquired either on a Bruker AMX 400 or a Bruker Avance 500 NMR spectrometer. Reaction mixtures were monitored on a Bruker Avance 200 NMR spectrometer. ^1H and $^{13}C\{^1H\}$ NMR spectra were referenced to external TMS by the residual proton resonances of the solvent (^1H) or the solvent itself (^{13}C). $^{11}B\{^1H\}$ NMR spectra were referenced to external $BF_3{\cdot}OEt_2$ and $^{31}P\{^1H\}$ NMR spectra to 85% H_3PO_4. Microanalyses for C, H and N were performed on a Leco CHNS-932 elemental analyser.

$[(OC)_4Mo(\mu\text{-}CO)\{\mu\text{-}BN(SiMe_3)_2\}Pd(PCy_3)]$ (16): Solid $[(OC)_5Mo{=}B{=}N(SiMe_3)_2]$ (**3**) (0.060 g, 0.147 mmol) was added to a pale yellow solution of $[Pd(PCy_3)_2]$ (**12**) (0.098 g, 0.147 mmol) in C_6D_6 (0.5 mL). After 5 min the reaction mixture was layered with hexane (2 mL) and stored at –35 °C. Over night orange crystals of $[(OC)_4Mo(\mu\text{-}CO)\{\mu\text{-}BN(SiMe_3)_2\}Pd(PCy_3)]$ (**16**) had formed (0.062 g, 53%). ^1H NMR (400 MHz, C_6D_6, 21 °C): δ = 1.97–1.14 (m, 33 H, Cy), 0.41 (s, 18 H, $SiMe_3$) ppm. $^{13}C\{^1H\}$ NMR (101 MHz, C_6D_6, 21 °C): δ = 213.0 (d, $J_{C,P}$ = 2 Hz, CO), 210.8 (d, $J_{C,P}$ = 4 Hz, CO), 34.0 (d, $^1J_{C,P}$ = 13 Hz, C^1, Cy), 31.5 (d, $^3J_{C,P}$ = 5 Hz, $C^{3,5}$, Cy), 27.8 (d, $^2J_{C,P}$ = 11 Hz, $C^{2,6}$, Cy), 26.5 (d, $^4J_{C,P}$ = 1 Hz, C^4, Cy), 3.8 (s, $SiMe_3$) ppm. $^{11}B\{^1H\}$ NMR (64 MHz, C_6D_6, 23 °C): δ = 99 (br. s, $\omega_{1/2}$ = 810 Hz) ppm. $^{31}P\{^1H\}$ NMR (162 MHz, C_6D_6, 21 °C): δ = 35.1 (s) ppm. IR (toluene): $\tilde{\nu}$ = 2043, 1962, 1939, 1876 [ν(C=O)] cm^{-1}. $C_{29}H_{51}BMoNO_5PPdSi_2$ (794.03): calcd. C 43.87, H 6.47, N 1.76; found C 43.77, H 6.47, N 1.72.

$[(Cy_3P)(OC)_3Mo(\mu\text{-}CO)\{\mu\text{-}BN(SiMe_3)_2\}Pt(PCy_3)]$ (19): Solid $[(OC)_5Mo{=}B{=}N(SiMe_3)_2]$ (**3**) (0.045 g, 0.110 mmol) was added to a pale yellow solution of $[Pt(PCy_3)_2]$ (**13**) (0.084 g, 0.110 mmol) in toluene (0.5 mL). The solution turned brown and then red. After 5 min the reaction mixture was layered with hexane (2 mL) and the solvent was allowed to slowly evaporate in the glovebox. The solid was extracted with C_6D_6, the red solution was layered with hexane (1.5 mL) and the solvent was allowed to evaporate. After 4 d pale red-brown crystals formed which were recrystallised from toluene/hexane yielding 15 mg (12%) of $[(Cy_3P)(OC)_3Mo(\mu\text{-}CO)\{\mu\text{-}BN(SiMe_3)_2\}Pt(PCy_3)]$ (**19**). ^1H NMR (500 MHz, C_6D_6, 27 °C): δ = 2.20–2.05 (m, 18 H, Cy), 1.80–1.58 (m, 30 H, Cy), 1.28–1.20 (m, 18 H, Cy), 0.63 (s, 18 H, $SiMe_3$) ppm. $^{13}C\{^1H\}$ NMR (126 MHz, C_6D_6, 27 °C): δ = 220.4 (d, $^2J_{C,P}$ = 2 Hz, CO), 220.3 (d, $^2J_{C,P}$ = 2 Hz, CO), 37.1 (d, $^1J_{C,P}$ = 13 Hz, C^1, Cy^{Mo}), 36.4 (d, $^1J_{C,P}$ = 22 Hz, C^1, Cy^{Pt}), 31.1 (d, $^3J_{C,P}$ = 2 Hz, $C^{3,5}$, Cy^{Pt}), 30.4 (s, $C^{3,5}$, Cy^{Mo}), 28.1 (d, $^2J_{C,P}$ = 10 Hz, $C^{2,6}$, Cy^{Mo}), 27.9 (d, $^2J_{C,P}$ = 11 Hz, $C^{2,6}$, Cy^{Pt}), 26.8 (s, C^4, Cy^{Mo}), 26.7 (s, C^4, Cy^{Pt}), 4.2 (s, $SiMe_3$) ppm. $^{11}B\{^1H\}$ NMR (160 MHz, C_6D_6, 27 °C): δ = 100 (br. s, $\omega_{1/2}$ = 1557 Hz) ppm; $^{31}P\{^1H\}$ NMR (202 MHz, C_6D_6, 27 °C): δ = 70.6 (d, $^4J_{P,P}$ = 11 Hz, $^1J_{P,Pt}$ = 5002 Hz, P^{Pt}), 49.9 (d, $^4J_{P,P}$ = 11 Hz, $^3J_{P,Pt}$ = 73 Hz, P^{Mo}) ppm. IR (toluene): $\tilde{\nu}$ = 1985, 1889, 1796, 1766 [ν(C=O)] cm^{-1}. $C_{46}H_{84}BMoNO_4P_2PtSi_2$ (1135.11): calcd. C 48.67, H 7.46, N 1.23; found C 48.54, H 7.11, N 1.20.

Crystal Structure Determination: The crystal data of **16** and **19** were collected on a Bruker X8APEX diffractometer with a CCD area detector and Mo-K_α radiation monochromated by using a multilayer mirror. The structures were solved by direct methods, refined with the Shelx software package (G. Sheldrick, University of Göttingen, 1997) and expanded using Fourier techniques. All non-hydrogen atoms were refined anisotropically. Hydrogen atoms were assigned to idealised positions and were included in structure factor calculations.

Crystal Data for 16: $C_{29}H_{51}BMoNO_5PPdSi_2$, M_r = 794.01, orange bar, 0.23 × 0.21 × 0.13 mm, orthorhombic space group $Pna2_1$, a = 17.7385(13) Å, b = 9.5613(7) Å, c = 21.3089(15) Å, V = 3614.1(5) $Å^3$, Z = 4, ρ_{calcd} = 1.459 $g\,cm^{-3}$, μ = 0.990 mm^{-1}, $F(000)$ = 1632, T = 173(2) K, R_1 = 0.0307, wR_2 = 0.0649, 7134 independent reflections [$2\theta \leq 52.24°$] and 370 parameters.

Crystal Data for 19: $C_{46}H_{84}BMoNO_4P_2PtSi_2$, M_r = 1135.10, yellow block, 0.19 × 0.10 × 0.07 mm, triclinic space group $P\bar{1}$, a = 12.2522(7) Å, b = 13.4914(8) Å, c = 16.2482(10) Å, α = 96.7280(10)°, β = 101.2180(10)°, γ = 96.7180(10)°, V = 2589.3(3) $Å^3$, Z = 2, ρ_{calcd} = 1.456 $g\,cm^{-3}$, μ = 3.088 mm^{-1}, $F(000)$ =

1164, T = 173(2) K, R_1 = 0.0462, wR_2 = 0.1017, 10261 independent reflections [$2\theta \leq 52.28°$] and 551 parameters.

CCDC-645809 and -645810 contain the crystallographic data for this article. These data can be obtained free of charge from the Cambridge Crystallographic Data Centre via www.ccdc.cam.ac.uk/data_request/cif

Supporting Information (see also the footnote on the first page of this article): Results of DFT calculations.

Acknowledgments

This work was supported by the Deutsche Forschungsgemeinschaft (DFG). The authors thank Dr. F. Seeler for performing the X-ray diffraction study of compound **19**.

[1] a) K. Burgess, M. J. Ohlmeyer, *Chem. Rev.* **1991**, *91*, 1179–1191; b) I. Beletskaya, A. Pelter, *Tetrahedron* **1997**, *53*, 4957–5026.
[2] T. B. Marder, N. C. Norman, *Top. Catal.* **1998**, *5*, 63–73.
[3] a) J.-Y. Cho, M. K. Tse, D. Holmes, R. E. Maleczka Jr, M. R. Smith III, *Science* **2002**, *295*, 305–308; b) T. Ishiyama, N. Miyaura, *J. Organomet. Chem.* **2003**, *680*, 3–11; c) T. Ishiyama, Y. Nobuta, J. F. Hartwig, N. Miyaura, *Chem. Commun.* **2003**, 2924–2925; d) D. N. Coventry, A. S. Batsanov, A. E. Goeta, J. A. K. Howard, T. B. Marder, R. N. Perutz, *Chem. Commun.* **2005**, 2172–2174; e) J. F. Hartwig, K. S. Cook, M. Hapke, C. D. Incarvito, Y. Fan, C. E. Webster, M. B. Hall, *J. Am. Chem. Soc.* **2005**, *127*, 2538–2552, and references therein.
[4] a) H. Braunschweig, *Angew. Chem.* **1998**, *110*, 1882–1898; *Angew. Chem. Int. Ed.* **1998**, *37*, 1786–1801; b) H. Braunschweig, M. Colling, *Coord. Chem. Rev.* **2001**, *223*, 1–51; c) H. Braunschweig, M. Colling, *Eur. J. Inorg. Chem.* **2003**, 393–403; d) H. Braunschweig, *Adv. Organomet. Chem.* **2004**, *51*, 163–192; e) H. Braunschweig, C. Kollann, D. Rais, *Angew. Chem.* **2006**, *118*, 5380–5400; *Angew. Chem. Int. Ed.* **2006**, *45*, 5254–5274; f) J. Uddin, C. Boehme, G. Frenking, *Organometallics* **2000**, *19*, 571–582; g) J. Uddin, C. Boehme, G. Frenking, *Coord. Chem. Rev.* **2000**, *197*, 249–276; h) J. Uddin, G. Frenking, *J. Am. Chem. Soc.* **2001**, *123*, 1683–1693.
[5] a) A. W. Ehlers, E. J. Baerends, F. M. Bickelhaupt, U. Radius, *Chem. Eur. J.* **1998**, *4*, 210–221; b) U. Radius, F. M. Bickelhaupt, A. W. Ehlers, N. Goldberg, R. Hoffmann, *Inorg. Chem.* **1998**, *37*, 1080–1090.
[6] a) P. L. Timms, *J. Am. Chem. Soc.* **1967**, *89*, 1629–1632; b) P. L. Timms, *Acc. Chem. Res.* **1973**, *6*, 118–123.
[7] H. Braunschweig, C. Kollann, U. Englert, *Angew. Chem.* **1998**, *110*, 3355–3357; *Angew. Chem. Int. Ed.* **1998**, *37*, 3179–3180.
[8] a) H. Braunschweig, D. Rais, K. Uttinger, *Angew. Chem.* **2005**, *117*, 3829–3832; *Angew. Chem. Int. Ed.* **2005**, *44*, 3763–3766; b) H. Braunschweig, K. Radacki, D. Rais, K. Uttinger, *Organometallics* **2006**, *25*, 5159–5164; c) H. Braunschweig, C. Burschka, M. Burzler, S. Metz, K. Radacki, *Angew. Chem.* **2006**, *118*, 4458–4461; *Angew. Chem. Int. Ed.* **2006**, *45*, 4352–4355; d) H. Braunschweig, K. Radacki, D. Rais, F. Seeler, *Angew. Chem.* **2006**, *118*, 1087–1090; *Angew. Chem. Int. Ed.* **2006**, *45*, 1066–1069; e) H. Braunschweig, M. Forster, K. Radacki, *Angew. Chem.* **2006**, *118*, 2187–2189; *Angew. Chem. Int. Ed.* **2006**, *45*, 2132–2134.
[9] a) H. Braunschweig, M. Colling, C. Kollann, H. G. Stammler, B. Neumann, *Angew. Chem.* **2001**, *113*, 2359–2361; *Angew. Chem. Int. Ed.* **2001**, *40*, 2298–2300; b) H. Braunschweig, M. Colling, C. Hu, K. Radacki, *Angew. Chem.* **2003**, *115*, 215–218; *Angew. Chem. Int. Ed.* **2003**, *42*, 205–208.
[10] a) H. Braunschweig, T. Herbst, D. Rais, F. Seeler, *Angew. Chem.* **2005**, *117*, 7627–7629; *Angew. Chem. Int. Ed.* **2005**, *44*, 7461–7463.
[11] a) H. Braunschweig, M. Colling, C. Kollann, K. Merz, K. Radacki, *Angew. Chem.* **2001**, *113*, 4327–4329; *Angew. Chem. Int. Ed.* **2001**, *40*, 4198–4200; b) B. Blank, H. Braunschweig, M. Colling-Hendelkens, C. Kollann, K. Radacki, D. Rais, K. Uttinger, G. R. Whittell, *Chem. Eur. J.* **2007**, *13*, 4770–4781.
[12] a) D. L. Coombs, S. Aldridge, C. Jones, D. J. Willock, *J. Am. Chem. Soc.* **2003**, *125*, 6356–6357; b) D. L. Kays (née Coombs), J. K. Day, L.-L. Ooi, S. Aldridge, *Angew. Chem.* **2005**, *117*, 7623–7626; *Angew. Chem. Int. Ed.* **2005**, *44*, 7457–7460; c) S. Aldridge, C. Jones, T. Gans-Eichler, A. Stasch, D. L. Kays (née Coombs), N. D. Coombs, D. J. Willock, *Angew. Chem.* **2006**, *118*, 6264–6268; *Angew. Chem. Int. Ed.* **2006**, *45*, 6118–6122; d) H. Braunschweig, K. Radacki, D. Rais, D. Scheschkewitz, *Angew. Chem.* **2005**, *117*, 5796–5799; *Angew. Chem. Int. Ed.* **2005**, *44*, 5651–5654 ; e) H. Braunschweig, K. Radacki, K. Uttinger, *Angew. Chem.* **2007**, *119*, 4054–4057; *Angew. Chem. Int. Ed.* **2007**, *46*, 3979–3982.
[13] a) H. Braunschweig, T. Wagner, *Angew. Chem.* **1995**, *107*, 904–905; *Angew. Chem. Int. Ed. Engl.* **1995**, *34*, 825–826; b) H. Braunschweig, C. Kollann, U. Englert, *Eur. J. Inorg. Chem.* **1998**, 465–468; c) H. Braunschweig, C. Kollann, K. W. Klinkhammer, *Eur. J. Inorg. Chem.* **1999**, 1523–1529.
[14] H. Braunschweig, K. Radacki, D. Rais, F. Seeler, K. Uttinger, *J. Am. Chem. Soc.* **2005**, *127*, 1386–1387.
[15] H. Braunschweig, K. Radacki, D. Scheschkewitz, G. R. Whittell, *Angew. Chem.* **2005**, *117*, 1685–1688; *Angew. Chem. Int. Ed.* **2005**, *44*, 1658–1660.
[16] a) J. F. Hartwig, S. R. DeGala, *J. Am. Chem. Soc.* **1994**, *116*, 3661–3662; b) J. F. Hartwig, X. He, *Organometallics* **1996**, *15*, 5350–5358.
[17] J. F. Hartwig, X. He, *Angew. Chem.* **1996**, *108*, 352–354; *Angew. Chem. Int. Ed. Engl.* **1996**, *35*, 315–317.
[18] a) H. Braunschweig, B. Ganter, M. Koster, T. Wagner, *Chem. Ber.* **1996**, *129*, 1099–1101; b) H. Braunschweig, K. W. Klinkhammer, M. Koster, K. Radacki, *Chem. Eur. J.* **2003**, *9*, 1303–1309 ; c) . H. Braunschweig, K. W. Klinkhammer, M. Koster, *Angew. Chem.* **1999**, *111*, 2368–2370; *Angew. Chem. Int. Ed.* **1999**, *38*, 2229–2231; d) H. Braunschweig, M. Koster, R. Wang, *Inorg. Chem.* **1999**, *38*, 415–416.
[19] S. W. Helm, G. Linti, H. Nöth, S. Channareddy, P. Hofmann, *Chem. Ber.* **1992**, *125*, 73–86.
[20] H. Wadepohl, U. Arnold, H. Pritzkow, *Angew. Chem.* **1997**, *109*, 1009–1011; *Angew. Chem. Int. Ed. Engl.* **1997**, *36*, 974–976.
[21] J. R. Graham, R. J. Angelici, *Inorg. Chem.* **1967**, *6*, 2082–2085.
[22] H. Braunschweig, K. Radacki, D. Rais, G. R. Whittell, *Angew. Chem.* **2005**, *117*, 1217–1219; *Angew. Chem. Int. Ed.* **2005**, *44*, 1192–1194.
[23] a) W. Kuran, A. Musco, *Inorg. Chim. Acta* **1975**, *12*, 187–193; b) S. Otsuka, T. Yoshida, M. Matsumoto, K. Nakatsu, *J. Am. Chem. Soc.* **1976**, *98*, 5850–5858.
[24] a) S.-Y. Onozawa, Y. Hatanaka, T. Sakakura, S. Shimada, M. Tanaka, *Organometallics* **1996**, *15*, 5450–5452; b) S.-Y. Onozawa, M. Tanaka, *Organometallics* **2001**, *20*, 2956–2958.
[25] R. H. Crabtree, M. Lavin, *Inorg. Chem.* **1986**, *25*, 805–812.
[26] Electronic structure calculations reported in this work were performed with *Gaussian 03, Revision B.04*, Gaussian, Inc., Pittsburgh PA, **2003**; The Electron Localisation Function and its properties were computed with the TopMoD package of S. Noury, X. Krokidis, F. Fuster, B. Silvi, **1997**; the charges and the Wiberg Bond Indices were calculated with the NBO 5 program of E. D. Glendening, J. K. Badenhoop, A. E. Reed, J. E. Carpenter, J. A. Bohmann, C. M. Morales, **2001**. See electronic supporting information for details on the computations.

Received: March 30, 2007
Published Online: July 27, 2007

